Quaternary Science Reviews 157 (2017) 14–28

Contents lists available at ScienceDirect

Quaternary Science Reviews

journal homepage: www.elsevier.com/locate/quascirev

Late Glacial to Holocene paleoenvironmental change on the northwestern Pacific seaboard, Kamchatka Peninsula (Russia)

Ionel Florin Pendea [a, *], Vera Ponomareva [b], Joanne Bourgeois [c], Ezra B.W. Zubrow [d], Maxim Portnyagin [e, f], Irina Ponkratova [g], Hans Harmsen [d], Gregory Korosec [d]

[a] Lakehead University, Sustainability Sciences Department, 500 University Avenue, Orillia, ON, L3V0B9, Canada
[b] Institute of Volcanology and Seismology, Piip Blvd. 9, Petropavlovsk-Kamchatsky, 683006, Russia
[c] University of Washington, Department of Earth & Space Sciences, Seattle, WA, 98195-1310, USA
[d] State University of New York at Buffalo, Department of Anthropology, 380 MFAC, Buffalo, NY, 14261, USA
[e] Helmholtz Centre for Ocean Research Kiel (GEOMAR), Wischhofstr. 1-3, 24148, Kiel, Germany
[f] V.I. Vernadsky Institute of Geochemistry and Analytical Chemistry, Kosygin Str. 19, Moscow, 119991, Russia
[g] North International University, Portovaya Str. 13, Magadan, 685030, Russia

ARTICLE INFO

Article history:
Received 2 May 2016
Received in revised form
9 November 2016
Accepted 28 November 2016

Keywords:
Kamchatka Peninsula
Late Glacial
Holocene
Pollen
Charcoal
Tephra
Vegetation history
Fire history

ABSTRACT

We used a new sedimentary record from a small kettle wetland to reconstruct the Late Glacial and Holocene vegetation and fire history of the Krutoberegovo-Ust Kamchatsk region in eastern Kamchatka Peninsula (Russia). Pollen and charcoal data suggest that the Late Glacial landscape was dominated by a relatively fire-prone *Larix* forest-tundra during the Greenland Interstadial complex (GI 1) and a subarctic steppe during the Younger Dryas (GS1). The onset of the Holocene is marked by the reappearance of trees (mainly *Alnus incana*) within a fern and shrub dominated landscape. The Holocene Thermal Maximum (HTM) features shifting vegetational communities dominated by *Alnus* shrubs, diverse forb species, and locally abundant aquatic plants. The HTM is further defined by the first appearance of stone birch forests (*Betula ermanii*) – Kamchatka's most abundant modern tree species. The Late Holocene is marked by shifts in forest dynamics and forest-graminoid ratio and the appearance of new non-arboreal taxa such as bayberry (*Myrica)* and meadow rue (*Filipendula).* Kamchatka is one of Earth's most active volcanic regions. During the Late Glacial and Holocene, Kamchatka's volcanoes spread large quantities of tephra over the study region. Thirty-four tephra falls have been identified at the site. The events represented by most of these tephra falls have not left evidence of major impacts on the vegetation although some of the thicker tephras caused expansion of grasses (Poaceae) and, at least in one case, forest die-out and increased fire activity.

1. Introduction

The Kamchatka Peninsula is located in the northwestern Pacific at the intersection of Arctic, Eurasian, and North American bioclimatic influences (Fig. 1) and is characterized by a highly diverse tectonic landscape. Similar to the North Atlantic region, environmental changes in and around the North Pacific following the Last Glacial Maximum about 20,000 years ago were large and rapid (Praetorius and Mix, 2014). The patterns of variation were complex, and the highly dynamic paleoclimatic and paleooceanograpic couplings between the two northern oceans led to both syn- and diachronicity (Yasuhara et al., 2012; Max et al., 2012; Praetorius and Mix, 2014). In the North Pacific, deglacial warming was mediated by the orbitally forced increase in summer insolation but also by linkages to deglacial variations in the Atlantic meridional overturning circulation (AMOC) and by close atmospheric couplings between the North Pacific and North Atlantic and between the North Pacific and the adjacent landmasses (Max et al., 2012). The latter coupling was probably dominated by the changing position and strength of the two pressure systems that drive the present day climate in the region: the Siberian High and the Aleutian Low (Mock et al., 1998). However, the patterns of deglacial warming, including the development of the Late Glacial cold reversal (the Younger Dryas), are poorly known especially from terrestrial records.

* Corresponding author.
E-mail address: ifpendea@lakeheadu.ca (I.F. Pendea).

http://dx.doi.org/10.1016/j.quascirev.2016.11.035
0277-3791/

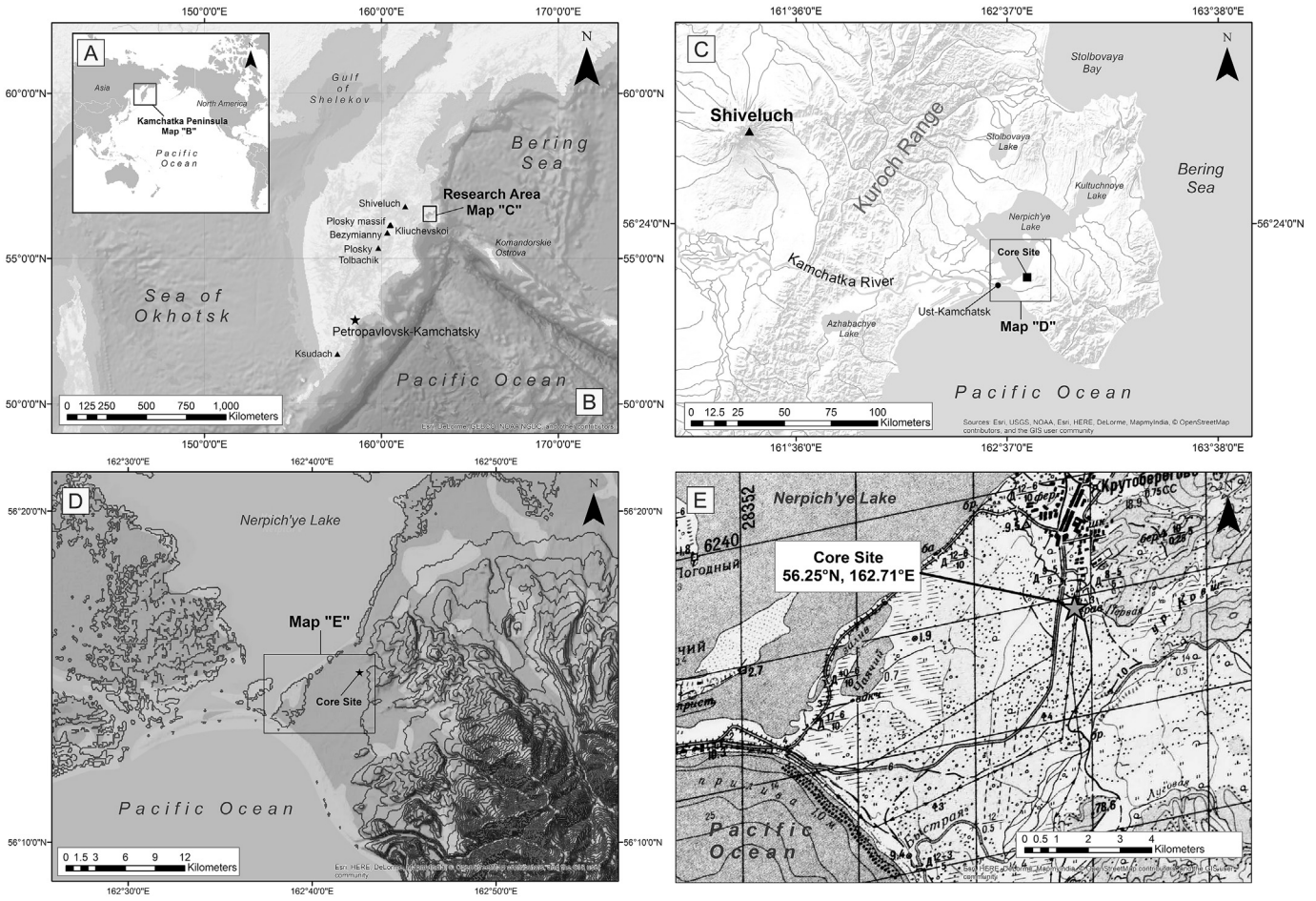

Fig. 1. Location Maps. A) the study region in the global context; B) Kamchatka Peninsula and the surrounding seas; C) detail of east-central Kamchatka; D) DEM detail of the core site near the transition between the Pacific Ocean and a coastal lagoon; E) topographic detail of the core site.

On the Kamchatka Peninsula, the patterns of deglacial paleoclimate and paleoenvironmental change are even less clear than elsewhere in the North Pacific. To date, there is no reliable information on Late Glacial paleoenvironments with the exception of some early studies, mostly in Russian, which report paleoenvironmental data with little to no age control (Neishtadt, 1957; Khotinsky, 1977; Braitseva et al., 2005). By comparison, Holocene paleoenvironments are relatively well documented. From north-central Kamchatka, Andrén et al. (2015), Hammarlund et al. (2015), and Self et al. (2015), among others, present new, high-resolution, multi-proxy lake records, while Nazarova et al. (2013) and Hoff et al. (2014) conducted single-proxy paleoenvironmental reconstructions in southern and central Kamchatka. In addition, recent reassessments of previous pollen-based reconstructions were undertaken by Dirksen et al. (2013). All these studies bring evidence of a highly variable Holocene climate. For instance, Nazarova et al. (2013) analyzed the chironomid remains in lake sediments from the Two-Yurts Lake in central Kamchatka and found a variable Late Holocene climate with four distinct climate periods. Hammarlund et al. (2015) used cellulose-inferred lake-water $\delta^{18}O$ to infer Holocene regional precipitation variability and long-term atmospheric circulation over easternmost Asia.

This paper aims to further our understanding of the Late Glacial to Holocene environmental history of Kamchatka. We use pollen and microscopic charcoal from a 7-m-long sediment sequence and 16 ^{14}C dates to reconstruct vegetation and regional fire dynamics in eastern Kamchatka near the Pacific Ocean - Bering Sea junction (Fig. 1). We specifically address the question of whether Kamchatka's Late Glacial paleoenvironments were similar to those of other locales in the northern hemisphere and, in particular, whether the region experienced the Late Glacial cold reversal known as the Younger Dryas. The existence of a region-wide Younger Dryas (GS1) in the North Pacific has been previously questioned (e.g., Anderson et al., 2002; 2003; Kokorowski et al., 2008). To improve the detection of patterns of climate change we compare our findings to previous paleoclimatic and paleoenvironmental records in the region. In addition, we present some evidence regarding the role of tephra falls from Kamchatka's large-scale explosive volcanism in postglacial vegetation dynamics.

2. General geographical setting

Kamchatka Peninsula (Fig. 1) is a boreal-subarctic landmass of almost 500,000 km^2 bordered by the Pacific Ocean to the east and south, Bering Sea to the northeast, and the Sea of Okhotsk to the west. To the north, a narrow land strip links the peninsula to the Koryak Highlands of southwestern Beringia. Kamchatka lies at the intersection of two opposing climatic influences, one continental subarctic (cold and dry) and one maritime subarctic (cold and wet). To the west, the cold maritime conditions of the Sea of Okhotsk and to the north, the orographic barrier of the Koryak Highlands moderate the influence of the vast continental subarctic landmass of NE Siberia. To the northeast, east and southeast strong cyclonic activity, particularly from the North Pacific, brings cool humid air

and high precipitation along Kamchatka's eastern and southern seaboard (Krestov, 2008). The Oyashio current, a cold subarctic current transporting frigid waters from the Arctic Ocean through the Bering Sea, is particularly influential on the east coast of Kamchatka where summers are short, cool, wet and cloudy, and winters are characterized by high snowfall and low temperatures (Krestov, 2008). Two longitudinal (north-south) orographic barriers through the center of the peninsula separate coastal regions dominated by a cold maritime climate from an interior tectonic depression characterized by more continental conditions.

As the Kamchatka Peninsula lies along a very active subduction zone (Eichelberger et al., 2007), the terrestrial environment is influenced by extensive volcanism. Approximately 30 active, explosive volcanoes, including the highest volcano in Eurasia (Kliuchevskoi), have produced a thick soil-pyroclastic cover over much of the peninsula (e.g., Braitseva et al., 1997). Typically, tephra layers have unique geochemical signatures, and extensive tephrochronological work undertaken by Braitseva et al. (1997), Kyle et al. (2011), Plunkett et al. (2015), and Ponomareva et al. (2013, 2015), among others, provides a good basis for both local and regional stratigraphic correlations.

2.1. The study site

The research site (56.25°N, 162.71°E, 19 m a.s.l.) is a small coastal peatland nested in a former kettle basin ~250 m in diameter situated on the outskirts of Krutoberegovo village, ~4 km from a sheltered coastal lagoon (Fig. 1). The kettle basin is exclusively rain fed and has no apparent surface drainage. The average annual temperature in the fieldwork area (Ust-Kamchatsk weather station, 56.2°N, 162.7°E, 4 m a.s.l.) is −0.33 °C and average precipitation is 718 mm/year. July and January average temperatures are 11.2 °C and −11.8 °C, respectively (Kondratyuk, 1974).

The vegetation of the study region is characterized by a strong altitudinal gradient (Krestov, 2008; Pendea et al., 2016). Below 500 m a.s.l., the vegetation is dominated by stone birch (*Betula ermanii)* woodlands, tall grasslands with Poaceae and tall forbs, and fen peatlands. Between 500 and 1000 m a.s.l. the landscape is dominated by shrub tundra with shrub alder (*Alnus fructicosa)* and at elevations higher than 1000 m a.s.l., the alder tundra is replaced by alpine sedge tundra, unvegetated mineral soils, and perennial snow. The study site is characterized by a *Myrica tomentosa*-Cyperaceae peatland community with a bryophyte understory dominated by Bryidae mosses and *Sphagnum teres.* Around the site, the vegetation comprises of species-rich communities dominated by *Alnus fructicosa* and tall forbs such as *Senecio canabifolius* and *Filipendula camtschatica.* The upland vegetation surrounding the wetland is composed of *Betula ermanii* stands with a tall herbaceous layer, composed mainly of *Aconitum maximum*, *Heracleum lanatum*, *Saussurea pseudotilesii*, *Geranium erianthum*, and *Equisetum hyemale*.

3. Materials and methods

3.1. Coring and dating

Four test cores, up to 708 cm long, were taken along a transect through the middle of the peatland with a 2.5-cm-diameter, 1-m long, split-barrel Eijkelkamp® auger and extensions (Eijkelkamp Inc., 2016). Near the longest test core, we excavated to a depth of 4 m and took paleoecological and tephra samples as monoliths from the excavation walls. From the base of that excavation, we continued down with a Russian peat corer, recovering material to a depth of 708 cm, from which we sampled the lower part of the section. Paleoecological samples were subsampled from monoliths and cores every 10 cm as well as below and above visible tephra layers. Sixteen AMS (Accelerated Mass Spectrometry) ^{14}C ages were measured by Beta Analytic Inc., 14 on terrestrial plant macrofossils and two on pollen aliquots separated from a silty-sand gyttja matrix (Table 1). The pollen aliquot separation procedure follows Neulieb et al. (2013). Quoted errors for ^{14}C measurements represent one relative standard deviation statistics (68% probability), and counting errors are based on the combined measurements of the sample, background, and modern reference standards. Radiocarbon ages were corrected for isotopic fractionation and were calibrated using the IntCal13 curve (Reimer et al., 2013) and the calculations were performed using the cubic spline fit (Talma and Vogel, 1993). Calibrated ranges are reported as two standard deviations (Table 1). The age-depth model (Fig. 2) was derived using the Bacon software (Blaauw and Christen, 2011), which divides a dated sequence into many short sections for which accumulation rates (in yr cm^{-1}) are modelled. The accumulation rate of any individual section "*i*" depends both on prior information and, to a certain degree, on the accumulation rate of the previous section (*i*-1). In this way, a "memory" of accumulation rate throughout time is obtained, aimed to reflect environmental conditions that might change gradually over time.

3.2. Pollen, spore and microscopic charcoal analyses

Pollen preparation followed standard procedures for glycerine samples (Moore et al., 1991). Treated samples were washed over a 125-μm sieve, and the material retained on a 6-μm sieve was used for analysis. A tablet containing a known concentration of exotic *Lycopodium* spores was added to each sample to allow calculation of pollen concentrations (Stockmarr, 1977). Pollen was identified using published keys (Faegri et al., 1989; Moore et al., 1991; Kapp et al., 2000). For Betulaceae and Asteraceae we followed Blackmore et al. (2003) and Punt and Hoen (2009), respectively. Previous studies from Kamchatka (Dirksen et al., 2013) have visually separated four *Betula* taxa (*Betula ermanii*, *Betula platyphylla*, *Betula exilis,* and *Betula* spp.). It is unclear on what basis this separation was made, but most research on *Betula* pollen separation into subgeneric taxa (e.g., Birks, 1968; Prentice, 1981; Mäkelä, 1996; Caseldine, 2001) refute the possibility of a meaningful discrimination among *Betula* species without morphometric analyses. As we observed large size variations of *Betula* pollen in our fossil record, particularly in samples younger than 8000 cal yr BP, we attempted to segregate shrub birch (*Betula nana* sensu lato) from tree birch based on published morphometric studies (e.g., Birks, 1968; Prentice, 1981; Mäkelä, 1996; Caseldine, 2001; Clegg et al., 2005). While we recognize that analogues from other areas may not be applicable to Kamchatka due to varying environmental and ecological conditions, the studies mentioned above show that *Betula nana* pollen is characterized by high morphometric similarity across the Northern Hemisphere (Birks, 1968; Prentice, 1981; Mäkelä, 1996; Clegg et al., 2005). To separate shrub birch pollen in our fossil record we used the recommended diameter to pore depth ratio (D/P) and pore depth measurements with thresholds of 8.5 and 2.5 μm for D/P and pore depth, respectively (Clegg et al., 2005). *Betula* grains with D/P above 8.5 and pore depth below 2.5 μm were identified as *Betula nana*-type. All other *Betula* grains were considered tree *Betula.* The recommended D/P ratio is based on reference materials from Alaska and Yukon and has tested successful in recognizing *Betula nana* grains in 80.1% of cases (Clegg et al., 2005). Grain diameter and pore depth of *Betula* pollen was measured in each sample under a × 1000 magnification with the Micron® USB 2.0 software. Grain diameter was defined as the distance from the inner margin of the pore wall to the outer margin of the opposite wall, with the grain in polar view (Ives, 1977; Clegg

Table 1
Radiocarbon age measurements and associated calendar age ranges (95% probability).

Sample name	BETA ID #	Depth (cm)	Material	Radiocarbon age (yrs BP)	2σ probability age range (cal yrs BP)	
					1st	2nd
JB112-45	320725	44–45	*Myrica tomentosa* twig	310 ± 30	300–470	n/a
JB112–96.5	320726	94.5–96.5	*Myrica tomentosa* twigs	1250 ± 30	1120–1270	1080–1110
JB112-145	305864	139.5–145	*Myrica tomentosa* seeds	1800 ± 30	1690–1820	1630–1660
JB112–208.5	320727	207.5–208.5	Cyperaceae leaf epidermis	2640 ± 30	2740–2780	n/a
JB112-260	320728	259–260	Cyperaceae leaf epidermis	3560 ± 30	3950–3960	3820–3920
JB112-304	320729	301.5–304	Cyperaceae leaf epidermis	4020 ± 30	4560–4570	4420–4530
JB112-334	305865	331.5–334	*Carex* spp. seeds	4140 ± 30	4560–4820	4540–4550
JB112-381	320730	380–381	Cyperaceae leaf epidermis	4710 ± 30	5530–5580	5440–5480
JB112-465	320731	464–465	Cyperaceae leaf epidermis	5590 ± 30	6430–6430	6300–6410
JB112-546	320732	545–546	*Betula ermanii* wood and bark	6210 ± 30	7220–7240	7140–7180
JB112–556.5	305866	555–556	*Alnus fructicosa* twig	6980 ± 40	7890–7930	7700–7880
JB112-616	320733	615–616	Cyperaceae leaf epidermis	8000 ± 40	8720–9010	n/a
JB112-660	294573	659–660	Cyperaceae leaf epidermis	8330 ± 50	9470–9250	9170–9140
JB112-670	305867	669–670	Pollen aliquot	9040 ± 50	10170–10250	n/a
JB112-683	320735	682–683	Gyttja	10080 ± 40	11400–11820	n/a
JB112-695	305868	694–695	Gyttja	11860 ± 200	13310–14110	n/a

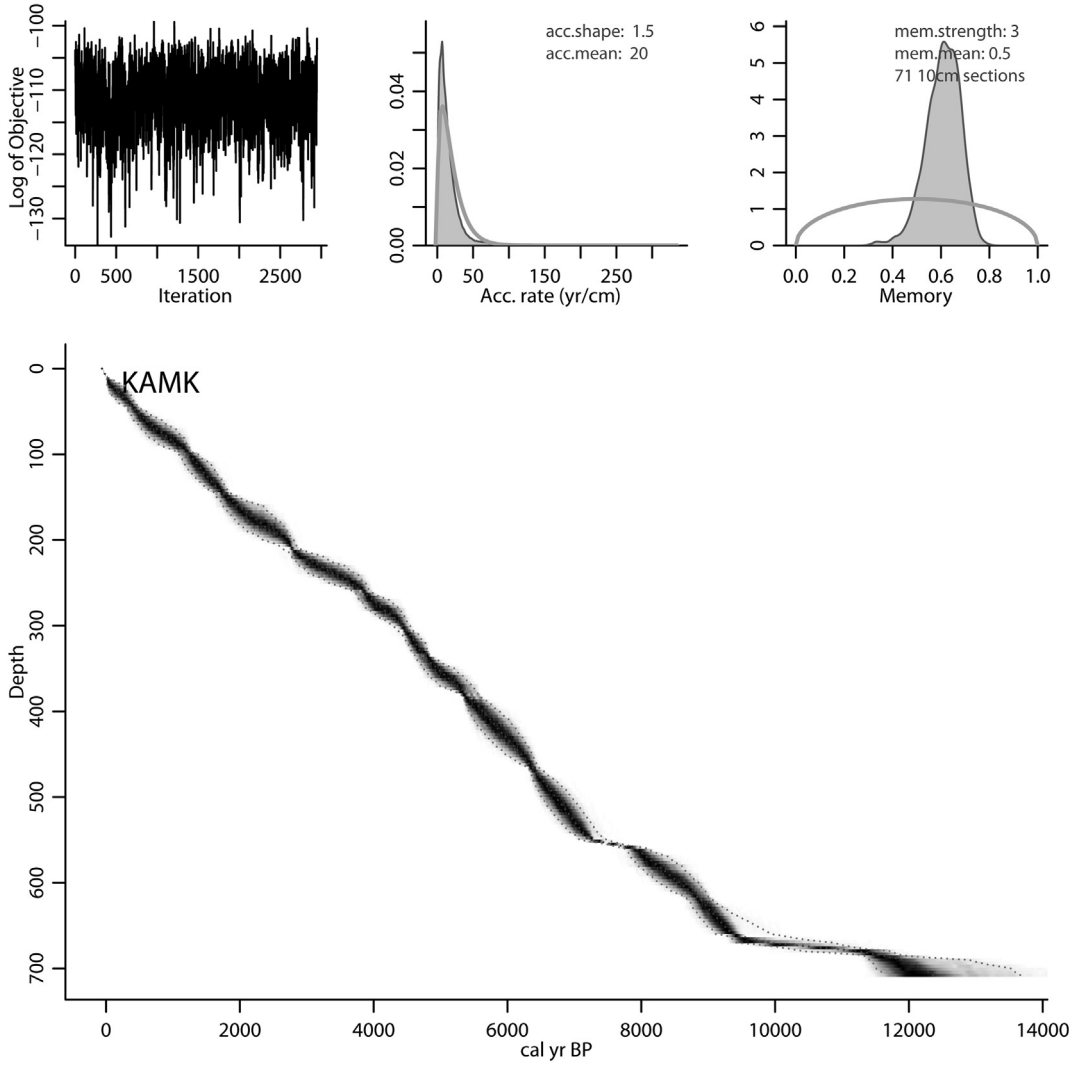

Fig. 2. The age-depth model based on radiocarbon dates and the age of a modern tephra (AD 1964) as constructed by the Bacon software (Blaauw and Christen, 2011). The shaded areas represent the 95% confidence interval of calendar ages. The model divides a dated sequence into many short sections for which accumulation rates (in yr cm^{-1}) are modelled. The accumulation rate of any individual section "*i*" depends both on prior information and, to a certain degree, on the accumulation rate of previous section (*i*-1). In this way, a "memory" of accumulation rate throughout time is obtained, aimed to reflect environmental conditions that might change gradually over time.

et al., 2005). Pore depth was defined as the distance from the outer margin of the sexine to the inner margin of the nexine across the vestibulum (Clegg et al., 2005). We attempted to measure at least 30 *Betula* grains in each sample. In samples where *Betula* counts were ≤30 grains we measured all grains that were not crumpled and visible in polar view.

More than 400 pollen grains were counted in all samples excluding aquatic pollen and spores, with counts ranging from 402 to 3024. For samples with high numbers of Cyperaceae pollen we counted at least 150 *Lycopodium* marker spores. Mean pollen counting resolution was 12 ± 7 cm or 255 ± 103 years. Together with pollen and spores from vascular plants we counted fossil sporangia of the mycorrhizal fungus *Glomus* spp. and used these as indicators of soil erosion following Anderson et al. (1984). The group Filicales includes all kidney-shaped monolete spores. Bryidae spore pollen group includes all moss spores that are typically <25 μm and circular or oval in polar view (see details in Moore et al., 1991; Brubaker et al., 1998).

Microscopic charcoal particles longer than 10 μm (or area >75 μm^2) were counted on pollen slides following Tinner and Hu (2003) and Finsinger and Tinner (2005). Charcoal number influx (particles $cm^{-2}yr^{-1}$) was estimated using the age-depth model and charcoal-particle concentration, the later estimated using the same approach as for pollen (Stockmarr, 1977).

3.3. Zonation and rate-of-change analyses

Both zonation and rate-of-change analyses were performed with the Psimpoll 4.27 program (Bennett, 2009). The pollen diagram was subdivided into local pollen assemblage zones (LPAZ) using constrained cluster analysis by sum-of-squares (CONISS) as developed by Grimm (1987). We identified seven LPAZ (Fig. 3) representing significant clusters according to the broken-stick method (Bennett, 1996). Subzones K-2a and K-2b correspond to CONISS clusters that were not statistically significant, but may be associated with an important ecosystem shift (see Discussion). Only taxa exceeding a threshold of 5% were included in the calculations following Birks and Berglund (1979) and Birks (1986). The analyses were carried out with untransformed datasets. Rate-of-change analysis was performed using the chord distance measure following Jacobson et al. (1987) and Jacobson and Grimm (1988).

3.4. Tephra description and analysis

Tephra samples used for geochemical analyses were extracted from monoliths and core material after shipment to Lakehead University, Canada. Microprobe analysis of all the tephras have been performed at GEOMAR Helmholtz Center for Ocean Research (Kiel, Germany) and the detailed results are presented in a separate paper. For the purpose of this paper, we focus on several marker tephras (see below) and include the observed and sampled tephras in the lithologic log (Table 2).

4. Results

4.1. Chronostratigraphy

All sixteen ^{14}C age (Table 1) estimates were accepted and allowed the construction of an age-depth model (Fig. 2). The oldest reliable chronology for the sediments extends to 14,500 cal yr BP. In the upper part of the sequence, in addition to the ^{14}C age estimates we included the absolute age of the historical SH1964 (AD 1964) marker tephra (Table 2). We identified this marker tephra based on its stratigraphic position, thickness, physical appearance, and glass composition similar to that found in the proximal deposits of this eruption (Ponomareva et al., 2015). The model shows a relatively uniform accumulation rate between 9500 cal BP and present. During this time almost 7 m of peat was deposited in the center of the kettle basin. The main lithostratigraphic units and the reconstructed sedimentary environments are detailed in Table 3. Between 709 and 685 cm the sediments are characterized by silty-sandy gyttja, likely deposited in a pond environment. The silty-sandy gyttja deposit is characterized by low accumulation rates, particularly between 11,500 and 9500 cal BP (Fig. 2). Between 685 and 620 cm the sediments are composed of mineralized sandy peat likely deposited in subaerial (dry) conditions. Above the sandy peat, the stratigraphy comprises of a succession of peat types as follows: sedge-carr peat (620-555 cm-depth), Bryidae-sedge peat (555-445 cm-depth), forest peat with abundant *Betula ermanii* wood fragments (445-405 cm-depth), Bryidae-sedge peat (405-225 cm-depth), and *Sphagnum*-sedge peat (225-0 cm-depth).

4.2. Tephra stratigraphy

The study area has experienced numerous tephra falls during Late Glacial to Holocene time. The section contains 34 distinct tephra layers ranging from 0.1 to 10 cm in thickness (Table 2). The majority of tephra layers are light-colored with a grain-size of very fine to medium sand. Several layers are coarse sand with a typical "salt-and-pepper" pattern caused by the presence of a large amount of plagioclases and dark minerals specific to Shiveluch eruptions (Braitseva et al., 1997). The section also contains a few layers of dark-gray and black, cindery, sand-sized tephra.

Based on thickness, distinct appearance, and area of dispersal, nine marker tephra layers present in the Krutoberegovo peat section are important for our study region and are highlighted in Table 2. These are from top to bottom: (1) coarse salt-and-pepper SH1964 tephra from the AD 1964 plinian Shiveluch eruption (Gorshkov and Dubik, 1970); (2) light-pale with grayish top, fine-grained KS_1 ash from Ksudach volcano (~1.7 cal ka; Braitseva et al., 1996, 1997; Pinegina et al., 2013); (3) coarse pumiceous SH#33 tephra from Shiveluch (4.5 ka); (4) normally graded (fine to medium-grained) yellow SHdv tephra from Shiveluch (~4.7 cal ka; Pevzner et al., 1998), (5) KS_2 tephra from Ksudach volcano (Braitseva et al., 1997); (6) SH#42 (~7.7 cal ka) and (7) SH#56 (~9.7 cal ka) tephras from Shiveluch volcano, (8) coarse-grained, black cindery PL2 tephra (~10.2 cal ka) positioned close to the bottom of the Holocene sequence (Ponomareva et al., 2013), and (9) SH#59 tephra (~10.8 cal ka), a beige-dull yellow fine sand tephra from the Shiveluch volcano. Estimates of tephra ages from the age-depth model are presented in Table 2 together with previous age estimates from the literature.

4.3. Pollen and microscopic charcoal

Pollen and spore percentages of all taxa and microscopic charcoal influx are presented in Fig. 3. Selected taxa are also presented as influx in Fig. 4 to permit the evaluation of taxa variability independent of each other. The pollen percentage diagram is divided into seven local pollen assemblage zones (LPAZ) as follows:

4.3.1. LPAZ K-1

The pollen assemblage characterizing the period before 12,300 cal yr BP (Fig. 3) is dominated by herbaceous taxa composed mainly of Cyperaceae (up to 50%) and Poaceae (up to 25%). Other common occurrences were Ranunculaceae (mainly *Thalictrum*), Saxifragaceae, and Asteraceae. Forbs from the poppy family (Papaveraceae) were briefly abundant. Among the aquatic and wetland taxa, *Sphagnum* and brown mosses (Bryidae) occur at high to moderate frequencies, *Potamogeton/Triglochin*-type at low

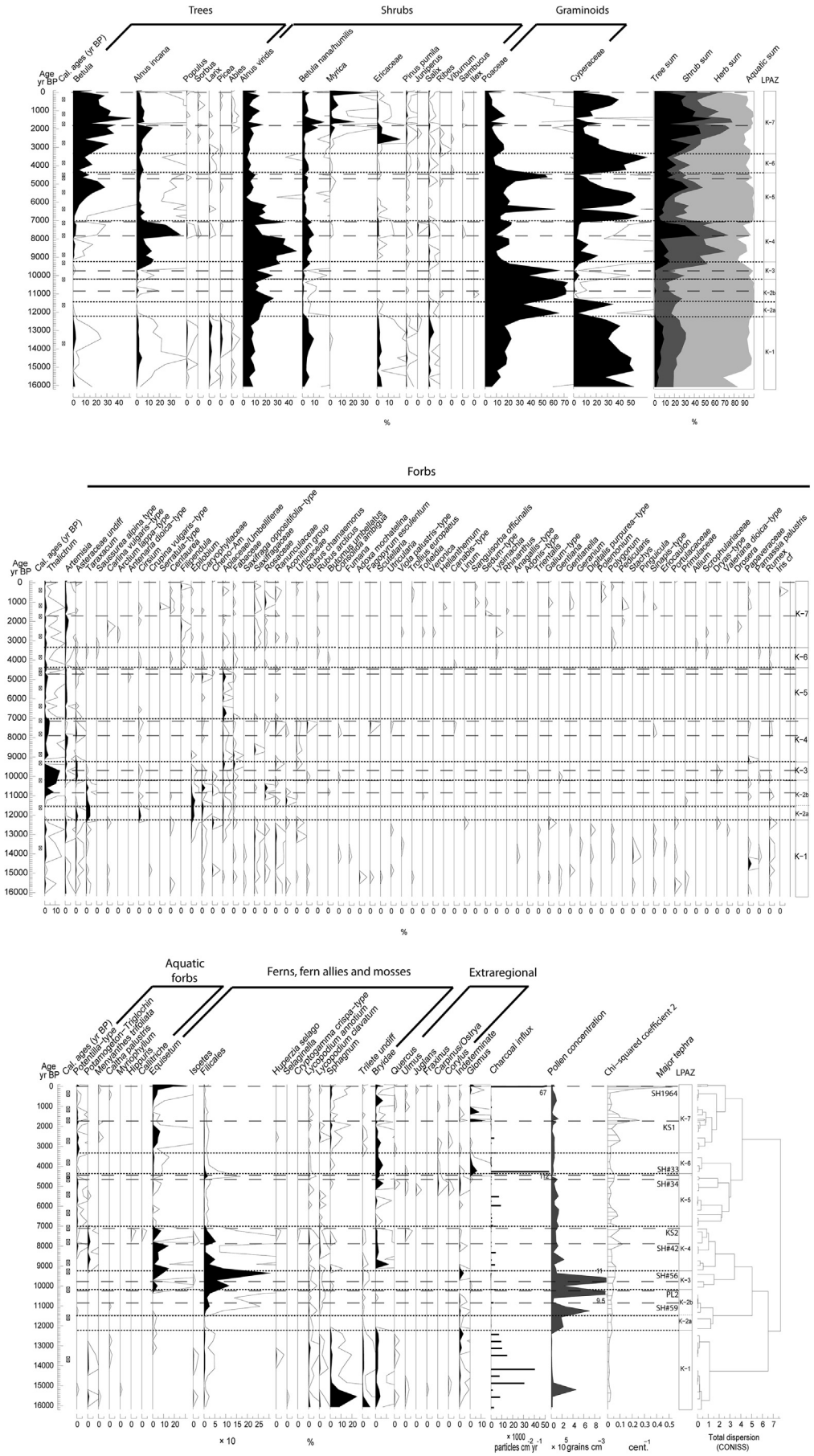

Fig. 3. Pollen percentages and charcoal influx diagram of Krutoberegovo wetland, eastern Kamchatka Peninsula, Kamchatsky Krai, Russia. Aquatic forbs, fern and fern allies, and mosses are excluded from the main sum. LPAZ – Local Pollen Assemblage Zones. Empty curves represent 10× exaggeration. Dashed lines mark the chronological position of major tephra deposition events highlighted in Table 2. Analyst: Florin Pendea.

frequencies and *Caltha palustris, Myriophyllum*, and *Isoetes* are rare. Shrub pollen, represented by *Alnus viridis, Betula nana/humilis,* Ericaceae, and *Salix* spp., accounts for 15–20% of the pollen spectra. Tree pollen types present were Larix (~0.5–3%), *Betula* spp. (≤2.5%), *Alnus incana* (~2–5%), and *Picea* (~1.5%), the latter probably derived from long-distance transport. Pollen concentration values are relatively low and complacent (<100,000 grains cm^{-3}) with the exception of one peak ca. 15,000 cal BP. The rate-of-change features some of the lowest chi-squared values in the sites' history. Relatively high and steady amounts of microscopic charcoal suggest a fire prone landscape during this period.

4.3.2. LPAZ K-2

The internal variability of zone K-2 (12,300–10,200 cal yr BP) warrants a further subdivision into two subzones: **K-2a** and **K-2b** (Fig. 3). In subzone **K-2a**, the pollen data show an absolute dominance of herbaceous pollen (Fig. 3). The most important taxon is now Poaceae, which increases its frequency to the detriment of formerly dominant Cyperaceae. An interesting development for this pollen subzone is the maximum occurrence of dandelion *(Taraxacum*) and thistle (*Cirsium)* and high frequencies of meadow-rue (*Thalictrum*), fireweed (*Epilobium),* and pinks (Caryophylaceae). Tree and aquatic/wetland pollen and spores all but disappear from the pollen spectra. Shrub taxa also decrease with the exception of *Alnus viridis*, which increases from ~10% to ~30%. The pollen assemblages of subzone **K-2b** feature the increasing dominance of grass pollen (Poaceae) which reaches an all time high (>70% of the main sum), almost completely replacing the sedge pollen (Cyperaceae). Another notable development in subzone K-2b is the reappearance of ferns (Filicales), which were virtually absent in subzone K-2a. LPAZ K-2 is characterized by variable pollen concentration with absolute values increasing almost an order of magnitude compared to LPAZ K-1. Rate-of-change values show little to no difference from those in LPAZ K-1. Charcoal is virtually absent throughout LPAZ K-2.

4.3.3. LPAZ K-3

The pollen assemblages of zone K-3 (10,200–9200 cal yr BP) are marked by a decrease in Poaceae and a progressive increase in tree alder (*Alnus incana*-type). Shrub pollen (mainly *Alnus viridis* and *Betula nana/humilis*) expands considerably towards the end of this zone reaching almost 50% of the pollen spectra. One of the most important features of this pollen zone is the advent of ferns (Filicales) and horsetails (*Equisetum*). The upland herbaceous pollen however remains largely unchanged, being dominated by Poaceae and *Thalictrum.* Pollen concentration reaches the highest values in the sites' history. In contrast, the rate-of-change shows a modest increase when compared to LPAZ K-2 suggesting a slow and/or progressive replacement of ecosystems. Microscopic charcoal is virtually absent throughout this zone indicating low fire activity.

4.3.4. LPAZ K-4

The period between 9200 and 7000 cal yr BP (LPAZ K-4) is marked by a profound change in the pollen and spore assemblages. As opposed to the previous two pollen zones, herbaceous pollen is no longer dominant and is largely replaced by shrub pollen, in particular *Alnus viridis*-type, *Betula nana/humilis* and *Salix.* The shrub pollen is also more diverse owing to the reappearance of *Ericaceae, Pinus pumila*, and *Juniperus*, which were largely absent between 12,300 and 9200 cal yr BP. The increase in tree pollen that commenced in LPAZ K-3 continues with a further increase in alder (*Alnus incana*-type) and the appearance of the first Holocene tree *Betula* pollen. Other tree pollen such as *Larix*, *Populus, Sorbus,* and *Picea* reappear in the pollen spectra but remain at frequencies <1.5%. Notable is also the reappearance of wetland and aquatic pollen (e.g., *Potamogeton/Triglochin*, *Potentilla*-type, *Hippuris*) as well as relatively high values of fern, horsetail, and Bryidae spores. Pollen concentration drops an order of magnitude in LPAZ K-4 compared to LPAZ K-3 and remains relatively stable through to LPAZ K-7. The rate-of-change values are similar to those of LPAZ K-4 with the exception of two moderate peaks, at 7200 and 7800 cal yr BP, which coincide with the deposition of tephra layers (Fig. 3). Micro-charcoal levels are low but slightly higher than in LPAZ K-3.

4.3.5. LPAZ K-5

The pollen record shows that shrub pollen decreased considerably around 7000 cal yr BP (Fig. 3), replaced by graminoid (Poaceae and Cyperaceae) and tree *Betula* assemblages. Early successional indicators (*Equisetum*, Filicales) almost disappear. Aquatic/wetland assemblages are now dominated by brown mosses (Bryidae) and marsh cinquefoil (*Potentilla).* The upper boundary of LPAZ K-5, dated ca. 4400 cal yr BP, is marked by strong decrease in tree (*Betula)* pollen and increase in grass pollen (Poaceae). This development corresponds with a brief (<200 years) increase in spores of Filicales and *Glomus,* and the deposition of Shiveluch tephras SH#34 and SH#33 at ca. 4700 and 4500 cal yr BP. The deposition of the two tephras is also marked by a slight increase in rate-of-change values. Micro-charcoal particle influx is rather low with the exception of two moderate peaks indicating some fire activity in the region.

4.3.6. LPAZ K-6

The pollen assemblages that characterize the end of LPAZ K-5 remain almost unchanged during LPAZ K-6 (4400-3300 cal yr BP) with the exception of widespread replacement of Poaceae with Cyperaceae and an increase in *Larix* pollen (Fig. 3). The most notable aspect of this pollen zone is the first appearance of *Filipendula* pollen, likely sourced from the moisture loving, thermophile tall herb *Filipendula camchatika*, a major constituent of the tall herb layer in modern vegetation of Kamchatka peninsula (Yakubov, 2007; Krestov, 2008). Pollen concentration and rate-of-change values show little change compared to LPAZ K-5. Micro-charcoal influx is low with the exception of one major peak possibly associated with the deposition of SH#33 tephra from Shiveluch.

4.3.7. LPAZ K-7

The pollen data for the last 3300 years document a substantial change in both wetland and upland assemblages at the site (Fig. 3). Noteworthy are the increase in tree *Betula* pollen, which reached their maximum frequencies (~50%) and an increase in shrubs from ~10% to >40%, both in the detriment of herbaceous pollen, which recedes to <35%. The increase in shrubland pollen is accompanied by the appearance and expansion of *Myrica*, and maximum Holocene expansion of Ericaceae and *Pinus pumila.* The herbaceous pollen is characterized by the co-dominance of Poaceae and Cyperaceae, a slight increase in *Artemisia,* and the reappearance of Saxifragaceae and Rosaceae. Pollen from the thermophile forb *Filipendula* reaches all-time highs at ca. 2500 and 300 cal yr BP. The wetland assemblages show an increase in *Sphagnum* spore frequencies, overall lower values of Bryidae spores, and the appearance of *Menyanthes trifoliata* pollen. Ferns all but disappear, but *Equisetum* reaches some of the highest frequencies in the site's history. Pollen concentration is similar to that of LPAZ K-6.

The rate-of-change data show two major peaks at ca. 1700 cal yr BP and AD 1964, coinciding with the deposition of two regionally important tephras (Fig. 3, Table 2). Fire activity is generally low with the exception of a charcoal peak likely associated with deposition of the Shiveluch SH1964 tephra.

Table 2
Tephra layers identified in the peat section at Krutoberegovo, (Russian Federation).

Tephra depth (cm)	Tephra code	Tephra Source	Age (cal BP) based on earlier estimates	Age (cal BP) based on the Krutoberegovo age-depth model	Thickness (cm)	Description
6.5–9	SH1964	Shiveluch	−14 (AD1964)	−14 (AD1964)	2.5	Salt-and-pepper medium sand
30–31	KL	Kliuchevskoi		227	1	Dark-gray very fine to fine sand
69	SH#8	Shiveluch	1073	765	0.5	Salt-and-pepper fine sand
94–96.5	SH#12 (SH1450)	Shiveluch	1403	1175	1	Salt-and-pepper reverse graded very fine to medium sand
114–115	KL	Kliuchevskoi		1404	1	Dark-gray fine sand
139–144	KS_1	Ksudach	1686 1785* 1742**	1725	5	Light-yellow-tan silt to very fine sand
153	SH#19a	Shiveluch	1742	1895	0.1	Salt-and-pepper fine sand
172.5–174	SH#21 (SH_5)	Shiveluch	1852 1951″	2194	1.5	Pale-yellow to salt-and-pepper reverse graded silt to fine sand
197	KL	Kliuchevskoi		2590	0.1	Dark-gray fine sand
208.5 −209.5	SH unit b (SH2800)	Shiveluch	3038 2906*** 3170″	2760	1	Beige-light-gray to salt-and-pepper reverse graded silt to fine sand
242.5–243	KL	Kliuchevskoi	3547″	3498	0.5	Dark-gray fine sand
259–259.5	SH#28 (SHsp)	Shiveluch	3959 3956″	3845	0.5	Dark-gray fine sand
265–266.5	SH#30	Shiveluch	4059	3943	1.5	Salt-and-pepper medium to coarse sand
280.5–281	SH#31?	Shiveluch	4109	4168	0.5	Light-tan very fine to fine sand
289	SH	Shiveluch	–	4285	0.1	Salt-and-pepper medium to coarse sand
296–296.7	SH#32	Shiveluch	4158	4387	0.7	Salt-and-pepper coarse sand
301.5 −303.5	SH#33	Shiveluch	4372	4495	2	Light-tan medium to very coarse sand
331.5 −333.5	SH#34 (SHdv)	Shiveluch	4892	4680	2	Light-yellow-tan silt to very fine sand
348–349	SH	Shiveluch	–	4925	1	Salt-and-pepper very fine to fine sand
380–381	SH#37	Shiveluch	5634	5450	1	Salt-and-pepper medium sand
384	SH + KL	Shiveluch + Kliuchevskoi	–	5488	0.2–0.3	Light-gray very fine sand
394	KL	Kliuchevskoi	–	5597	0.2	Black very fine to fine sand
405	KL	Kliuchevskoi	–	5717	tiny lense	Dark-gray silt
525	KL	Kliuchevskoi	–	6933	tiny lense	Pale silt
539–541	KL	Kliuchevskoi	–	7083	2	Dark-gray fine sand
546	KS_2	Ksudach	6886 6847** 7287^	7204	0.3	Greenish-gray very fine to fine sand
555.5 −556.5	SH#42	Shiveluch	7727	7780	1	Salt-and-pepper medium sand
610–611	SH#47	Shiveluch	8498	8756	0.1–0.2	Salt-and-pepper medium to coarse sand
654–655	SH#48	Shiveluch	8703	9300	1	Gray very fine to coarse sand
659–660	SH#54	Shiveluch	9685	9320	1	Gray very fine to coarse sand
660–664	SH#56	Shiveluch	9916	9700	4	Yellow medium sand
664–670	PL2	Plosky volcanic massif	10200****	10178	6	Dark-brownish-gray coarse sand
670–677	SH#59	Shiveluch	10741	10802	9	Beige - dull-yellow fine sand
682–683	PL1	Plosky volcanic massif	11650****	11556	1	Black very fine sand

Notes: Major marker tephras discussed in the paper are highlighted in gray. Identified tephras are labeled according to Braitseva et al. (1997) and Ponomareva et al. (2013, 2015). Shiveluch tephras are labeled SH followed with the number of the unit (Ponomareva et al., 2015); earlier published codes for several tephras are given in brackets. SH and KL are labels for non-identified Shiveluch and Kliuchevskoi tephras, respectively. identification of tephra layers is based on microprobe analyses and age estimates. Most of the ages in column 3 are from Ponomareva et al. (2015); ages marked with ” are based on the dates from Izvilisty site (Pendea et al., 2016); other ages are median probabilities of calibrated radiocarbon dates from Pinegina et al. (2013) (*); Braitseva et al. (1997) (**), Pevzner et al. (1998) (***), Ponomareva et al. (2013) (****), and Plunkett et al. (2015) (^).

5. Discussion

5.1. Vegetation history and potential paleoclimate relationships

Only few paleosites document a complete Late Glacial to Holocene environmental history in western Beringia (e.g., Lozhkin et al., 1993, 2011), and in Kamchatka the dataset presented here is to our knowledge the only one offering information on Late Glacial paleoenvironmental change. By comparison, Holocene vegetation dynamics are well documented (recent studies in the 2015 Global and Planetary Change special issue cited herein and a review of previous literature by Dirksen et al., 2013). The existing information on Kamchatka's Holocene paleoenvironments allows a comprehensive analysis of regional patterns of change. For the Late Glacial,

Table 3
Sedimentology.

Depth (cm)	Sediment type	Reconstructed sedimentary environment	Age (cal yr BP)
0–225	*Sphagnum*-sedge peat	Intermediate shrub-fen with *Myrica tomentosa* and Ericaceae	−60 to 3118
225–405	Bryidae-sedge peat	Rich fen	3118 to 5717
405–445	forest peat	*Betula ermanii* woodland with *Equisetum hyemale*	5717 to 6153
445–555	Bryidae-sedge peat	Rich fen	6153 to 7815
555–620	Sedge-carr peat	Rich shrub fen with *Alnus fructicosa*	7815 to 8910
620–685	mineralized sandy peat	Soil? (subaerial)	8910 to 12,045
685–709	silty-sandy gyttja	Pond	>12,045

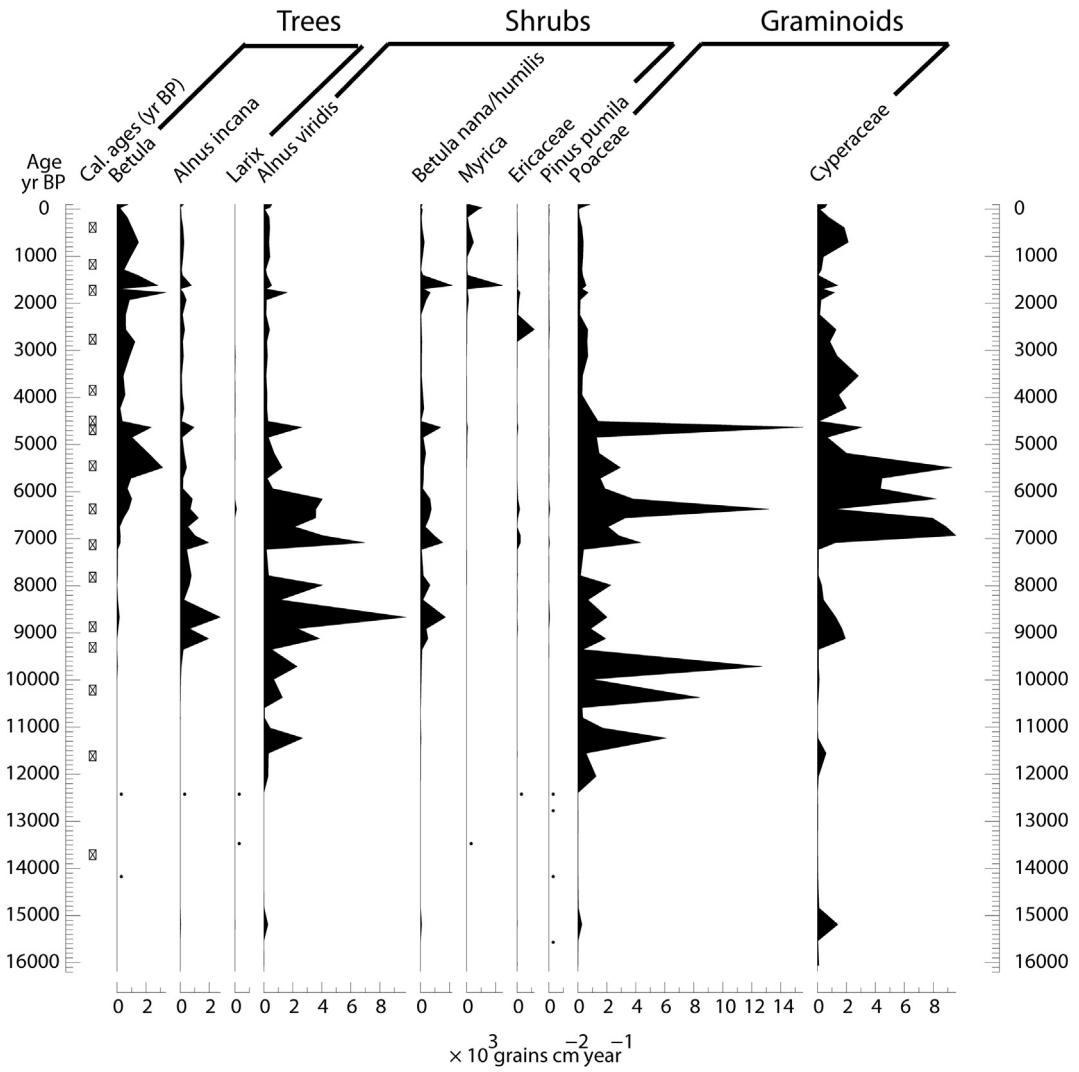

Fig. 4. Pollen influx diagram of Krutoberegovo wetland, eastern Kamchatka Peninsula, Kamchatsky Krai, Russia. Selected taxa only. Dots represent <1000 grains cm^{-2} yr^{-1}.

however, meaningful comparisons can only be made within a North Pacific context because well-dated Late Glacial stratigraphies are not available for the peninsula.

The Krutoberegovo locality provides the easternmost paleoenvironmental record for the Late Glacial to Holocene period in Kamchatka, and because of its near sea level elevation and position on the geographical boundary between the Bering Sea and the North Pacific proper, it exhibits some paleoenvironmental features that may be more similar to southwestern Alaska than to the rest of Kamchatka or to mainland northeast Asia. To allow for comparison between this study and well-constrained chronologies for the Northern Hemisphere we use the revised Greenland GICC-05 terminology (Rasmussen et al., 2006) together with the more generic Late Glacial to Holocene nomenclature suggested by Björck et al. (1998) and Walker et al. (2012) as follows:

5.1.1. The Late Glacial interstadial complex (GI 1, 14,700–12,650 cal yr BP)

A radiocarbon age estimate of 11,860 ± 200 yr BP (13,310–14,110 cal yr BP; Beta-305868) measured 12 cm above the core base indicates that the oldest sediments sampled were deposited during the Late Glacial interstadial complex GI 1. Sedimentation was dominated by mineral materials and likely took place in a shallow pond, while the surrounding landscape was dominated by forest-tundra/boreal woodland vegetation with a relatively diverse shrub component (*Betula nana/humilis*, Ericaceae, *Salix,* and *Pinus pumila*) and an herbaceous layer composed mostly of sedges (Cyperaceae). The relatively high proportion of *Sphagnum* spores may indicate high atmospheric humidity and the presence of bogs in the vicinity. This landscape appears to be unique to this stage and probably indicates a relatively warm Late Glacial climate. The reconstructed forest tundra/boreal woodland vegetation is indicated by the presence of *Larix* pollen in low but significant proportions (0.5–3%). This interpretation is supported by studies on surface pollen representation across the Russian Arctic (e.g., Jankovská et al., 2006) indicating strong underrepresentation of *Larix* pollen compared to its occurrence on the landscape. The presence of *Larix* trees – a taxon that was, and still is, confined to Kamchatka's more continental interior (Dirksen et al., 2013) – suggests that the climate of Kamchatka's eastern seaboard at this time was more continental than during the Holocene. Relatively high fire activity (Fig. 3) on the landscape brings further support to a continental climate during this time. The increased continentality during the Late Glacial in Kamchatka could be related to North Pacific paleogeography. According to Elias et al. (1997) and Keigwin et al. (2006) radiocarbon dates from the nearby Chukchi Sea

sediments place the submergence of the Beringian Land Bridge at ca. 12 ka cal BP. The presence of the land bridge and depressed sea levels in the North Pacific prior to 12 ka cal BP could have indeed created more continental conditions in western Beringia including Kamchatka.

An interesting floristic feature for this period is the brief but abundant appearance of poppies (Papaveraceae) between 14,500 and 15,000 cal yr BP, synchronous with a reduction in aquatic plant pollen and spores. It is unclear if such a vegetation development has a climatic significance, but wherever poppies have been identified in pollen records they seem to be associated with dry and cold grassland conditions (Tarasov et al., 1998; Lozhkin et al., 2001). In northeastern Siberia, for instance, poppies appear in more than trace amounts only during the Late Glacial (Anderson et al., 2002) indicating a cold and dry steppe biome. We suggest that in the Krutoberegovo record this brief poppy episode could correspond to a cool and dry phase. The decline of arboreal and shrubland vegetation and the expansion of grassland (Fig. 3) at ca.12,650 cal yr BP signals the end of GI 1.

5.1.2. The Late Glacial cold reversal or "Younger Dryas" in Kamchatka (GS 1, 12,650–11,500 cal yr BP) – an anomaly for northeast Asia?

Paleoclimatic research from northeast Asia and Beringia reveals complex patterns related to the nature and timing of the Younger Dryas (GS-1). Almost all Late Glacial records from northeast Asia reconstruct a quasi-continuous warming from the Last Glacial Maximum (LGM) through to the Early Holocene (Anderson et al., 2002; Kokorowski et al., 2008; Lozhkin et al., 2011a,b). In fact, some sites from the interior and northern parts of Alaska (Anderson et al., 2003) and from the northern Far East (Wrangel Island) (Lozhkin et al., 2011a,b) report warmer and/or wetter than present conditions during the Younger Dryas, which are at odds with the often dramatic cold reversal widely recognized elsewhere in the Northern Hemisphere (e.g., Mathewes, 1993; Peteet et al., 1993; Peteet, 1995). In other parts of Beringia (e.g., northern Alaska, northwestern Canada) evidence for a cooling during the Younger Dryas has been equally absent (Anderson et al., 2002; Kokorowski et al., 2008). These records are in stark contrast to paleoenvironmental reconstructions from the coastal regions of the North Pacific, in particular southern Alaska, which document a substantial cold reversal similar to and broadly contemporaneous with the GS1 in the North Atlantic region (Peteet and Mann, 1994; Mann and Hamilton, 1995; Brubaker et al., 2001). A similar climate event, albeit less pronounced, was identified south of Kamchatka on the Sakhalin Island of the Russian Far East (Igarashi and Zharov, 2011).

The Krutoberegovo record provides evidence that a cold reversal similar to Younger Dryas has also affected Kamchatka's North Pacific shoreline. The pollen evidence in this study indicates a marked floristic change between ca. 12,500 and 11,500 cal yr BP, corresponding to the end of LPAZ K-1 and LPAZ K-2a (Fig. 3). The forest-tundra/boreal woodland extant during GI 1 was replaced by a shrub steppe composed almost exclusively of grasses (Poaceae), dandelion (*Taraxacum*), thistles (*Cirsium*), asters (*Asteraceae*), fireweed (*Epilobium*), pinks (Caryophylaceae) and shrub alder (*Alnus viridis*), the latter as the only major remnant of the interstadial flora. Some of these vegetation constituents (e.g., dandelion, fireweed, and thistles) are almost exclusive to this period, while others such as meadow rue (*Thalictrum*) – a mostly temperate taxon with a quasi-continuous occurrence at this site – disappeared completely during this time (Fig. 3). An interesting floristic detail for this period is the temporary disappearance of ferns (Filicales) which otherwise exhibit a variable but continuous signal in the Krutoberegovo record. A similar development was observed by Peteet and Mann (1994) on Kodiak Island (southwestern Alaska) who suggestively named it "the Fern Gap". Noteworthy is also the disappearance of aquatic and wetland pollen and spores, which suggests that the pond might have completely dried out. This interpretation is supported by evidence of a change in the depositional environment from silty-sandy gyttja to mineralized sandy peat around 12,000 cal yr BP.

5.1.3. Early Holocene (11,500–9200 cal yr BP)

The onset of the Holocene in the Krutoberegovo record was marked by rather modest floristic changes. Alder trees (*Alnus incana*) reappeared around the site albeit in small numbers. Shrub communities (*Alnus viridis* and *Betula nana/humilis*) remained relatively unchanged during this period except towards the end when they seem to have expanded considerably. The herbaceous vegetation remained dominated by grasses, but became more diverse through the reappearance of meadow rue (*Thalictrum*), which expanded progressively to an all-time high around 9500 cal yr BP, and an increase in the abundance of Umbelliferae and legumes (Fabaceae). One of the most significant floristic changes marking the onset of the Holocene was the advent of ferns (Filicales), which grew rapidly in abundance, reaching a maximum at ca. 9200 cal yr BP. This vegetation development suggests a warmer and wetter climate during the early Holocene than in the previous period although vegetation reconstruction alone is insufficient for such an inference. The deposition of highly mineralized peat (soil?) during this time suggests that the core site surface may have frequently dried out.

The patterns of change in our record are, however, strikingly similar to those from a small coastal lake (Pechora Lake) from northeastern Kamchatka (Andrén et al., 2015). The Pechora Lake record begins ca. 10,000 cal yr BP and features an early Holocene with a similar floristic composition dominated by shrub alder (*Alnus viridis*), ferns (Filicales) and grasses. The only notable difference is the abundance of birch (*Betula*), higher at the Pechora Lake site than at Krutoberegovo, but a straightforward comparison is not possible as Andrén et al. (2015) do not differentiate tree birch from shrub birch.

5.1.4. The Holocene Thermal Maximum (9200 -4500 cal yr BP)

The Holocene Thermal Maximum (HTM) was a relatively warm period that is commonly associated with the orbitally forced Holocene maximum summer insolation (e.g., Berger, 1978; Bartlein et al., 2011). Its timing varies widely from region to region but is generally detected in paleorecords between 11 and 5 cal ka BP (e.g., Kaufman et al., 2004; Bartlein et al., 2011; Renssen et al., 2012). For instance, the onset of the HTM was delayed until 8 cal ka BP in northwestern Europe (Renssen et al., 2012).

In Kamchatka, the timing of the HTM varies. Dirksen et al. (2013) find warmer-than-present conditions between 9000 and 5000 cal yr BP in central Kamchatka and between 7000 and 5800 cal yr BP at coastal sites. At Pechora Lake, on the northeast coast, Andrén et al. (2015) detect a period of decreased lake ice cover and increased primary production starting at ca. 9600 cal yr BP. The same study, however, suggests that true HTM conditions were achieved only between ca. 6300 and 4500 cal yr BP as indicated by increased thermal lake stratification and high C/N ratio and $\delta^{18}C$ values.

At Krutoberegovo the HTM exhibits a complex pattern with substantial reorganisation of vegetation communities that may suggest variable climatic parameters during this time. Beginning at ca. 9200 cal yr BP the pollen record suggests a marked collapse of herbaceous communities concomitant with a strong expansion of shrubs, which reached an all-time high during this period. The dominant taxon is shrub alder (*Alnus viridis*), which probably formed quasi-continuous thickets around the site. The deposition

of sedge-carr peat between 8900 and 7800 cal yr BP suggests that *Alnus* shrubs might have also covered the core site surface. Tree taxa also expanded considerably, from almost absent in the Early Holocene to ~45% of the pollen spectra at ca. 7600 cal yr BP. The main representative is alder (*Alnus incana*), but a notable development is the first Holocene appearance of birch trees (*Betula* spp.). A radiocarbon age estimate of ca 7000 cal yr BP (6210 ± 30 ^{14}C yr BP; Beta-320732) obtained from a stone birch (*Betula ermanii*) branch indicates the earliest known Holocene occurrence of this tree in Kamchatka. Prior to the increase in tree birch (*Betula* spp.), a substantial increase of aquatic and wetland taxa (e.g., *Potamogeton/ Triglochin, Equisetum,* Bryidae) and a change in the depositional environment from sedge-carr peat to Bryidae-sedge peat around 7800 cal yr BP (Table 3) indicates that the core site became wetter potentially in response to a shift toward a more oceanic climate. This interpretation is further supported by changes in the upland vegetation, namely the reappearance of heaths (Ericaceae) and high proportions of ferns (Filicales) and horsetails (*Equisetum*).

Around 7000 cal yr BP there is a sharp shift in vegetation characterized by a decline in alders (both shrub and tree) and a corresponding increase in graminoids, in particular sedges (Cyperaceae). The forest vegetation is marked by a replacement of *Alnus incana* with *Betula* spp., which increased gradually and after 6000 cal yr BP became the dominant non-herbaceous taxa. Within the upland herb communities, Umbelliferae increased considerably and seem to have attained an ecological optimum during this time. The relative demise of wetland and humidity loving vegetation (*Potamogeton/Triglochin, Equisetum*, Filicales, Bryidae) and a shift in the depositional environment from Bryidae-sedge peat to forest peat, with abundant *Betula ermanii* macrofossils (Table 3), suggests that the rich fen might have become a woodland. The woodland episode, however, was brief as the site returned to rich fen conditions around 5700 cal yr BP (Table 3). A rise in Bryidae spores, particularly after ca. 5000 cal yr. BP brings support to this interpretation.

5.1.5. Late Holocene (4500 cal yr BP to present)

Previous pollen records are broadly in agreement that starting ca. 4500 cal yr BP the Kamchatka Peninsula underwent a general cooling (Dirksen et al., 2013; Meyer et al., 2014; Hammarlund et al., 2015; Andrén et al., 2015; Self et al., 2015) probably in connection with a global climate reorganisation towards cooler and drier conditions across mid- to low-latitude regions (Walker et al., 2012). The regional atmospheric circulation during this time was characterized by changes in the position and strength of the Siberian High (SH) and the Aleutian Low (AL). For instance, climate inferences based on lake proxies (Hammarlund et al., 2015) reconstruct mild and snow rich winters between 5000 and 3000 cal yr BP. The authors postulate that these climatic conditions were generated by the strengthening and northward migration of the SH and strengthening of the AL which generated a prevalence of northeasterly winds on the eastern coast of Kamchatka. Most studies recognize, however, a period of relative warmth within a general cooling trend, but the timing of this period differs among authors. For instance, Hammarlund et al. (2015) reconstruct warmer conditions with reduced winter snow after 2000 cal yr BP, while Nazarova et al. (2013) reconstruct higher summer temperatures between 3600 and 2800 cal yr BP. A more complex image of Late Holocene climate variability, inferred from pollen analysis, is presented by Dirksen et al. (2013), who recognize a time-transgressive warm phase starting from the east coast around 5200 cal yr BP, to the central Kamchatka depression at 3200 cal yr BP, and finally to the western lowlands where warmer conditions were reconstructed between 1900 and 1700 cal yr BP.

At Krutoberegovo, the Late Holocene vegetation changes demonstrate a degree of complexity marked by shifts in forest dynamics and forest-graminoid ratio and the appearance of new non-arboreal taxa such as *Myrica* and *Filipendula.* Between 5000 and 4500 cal yr BP the record shows a marked decline in tree birch (*Betula* spp.), while all other tree and shrub taxa proportions remain relatively unchanged. The birch decline, however, seems to be associated with a brief but strong increase in grasses (Poaceae) and an equally strong decrease in sedges (Cyperaceae). The brevity of this floristic development and the fact that it corresponds to the deposition of two major volcanic ashes at ca. 4700 and 4500 cal yr BP (Fig. 5), may indicate a disturbance-related process (see discussion in section 5.2). However, the abundance of birch tree pollen remains depressed until ca. 3000 cal yr BP, possibly under the influence of the Neoglacial cooling trend documented throughout Kamchatka (Meyer et al., 2014; Andrén et al., 2015; Self et al., 2015). After 3000 cal yr BP birch forests re-expanded progressively, reaching maximum proportions at ca.1500 cal yr BP. This maximum birch episode could have been caused by warmer summers and reduced winter snow. The birch maximum is, however, short lived as birch forest exhibited a continuous decline from 1500 cal yr BP to the present.

The non-arboreal vegetation exhibits several notable and potentially significant changes including the appearance of taxa that were not previously recorded at this site. The late Holocene vegetation record at Krutoberegovo features the appearance and dramatic expansion of bayberry (*Myrica*) at ca. 3000 cal yr BP and the expansion of heaths (Ericaceae), which together with the expanding birch forests may have replaced much of the mid Holocene graminoid-shrub landscape mosaic. This marked vegetational shift is also reflected in the nature of the peat deposited at the core site. Around 3100 cal yr BP the rich fen extant since ca. 5700 cal yr BP changes into an intermediate fen, with *Sphagnum* mosses and abundant remains of *Myrica tomentosa* and Ericaceae. The first appearance of the thermophile forb *Filipendula* (meadowsweet, dropwort) is recorded at 4500 cal yr BP with maximum values at ca. 2900-2000 and 300-200 cal yr BP. *Filipendula* is one of the most typical tall forbs in the current vegetation of Kamchatka, with preference for moist forest floor, river bank and wetland margin habitats and an altitudinal spread of up to 1000 m a.s.l. into the subalpine zone (Yakubov, 2007). However, its climatic significance is not straightforward. Clearly, it requires high soil humidity and in the Krutoberegovo paleorecord, the highest values of *Filipendula* pollen are indeed associated high values of aquatic and wetland taxa (Equisetum, *Potentilla*-type, and Sphagnum). Some authors (Klimaschewski, 2010) suggest that the expansion of *Filipendula* in the paleorecord of southern Kamchatka is related to warming. At Krutobetregovo, the proportion of *Filipendula* pollen is modest (<5%) and broadly corresponds with increases in cool oceanic indicators such as bayberry (*Myrica*), heaths (Ericaceae), and dwarf birch (*Betula nana*). However, the main peak in *Filipendula* pollen between 2900 and 2000 cal yr BP is synchronous with the maximum expansion of birch (*Betula* spp.) forests, which may indicate warmer conditions within a generally cool and humid Late Holocene.

The first Holocene appearance of dwarf pine pollen *(Pinus pumila*) at ca. 3000 cal yr BP, with values above background, suggests a shift towards thicker, longer-lasting snow cover (Krestov, 2008). Elsewhere in Kamchatka, the expansion of dwarf pine took place earlier (ca. 5000-4000 cal yr BP) and has been related to an intensification of the Siberian High, to short summers and long snowy winters (Andrén et al., 2015; Hammarlund et al., 2015). The later and much less dramatic increase in *Pinus pumila* on the eastern seaboard of Kamchatka suggests that the influence of the Siberian High in the Late Holocene of Kamchatka may have been mostly confined to central and eastern parts of the peninsula.

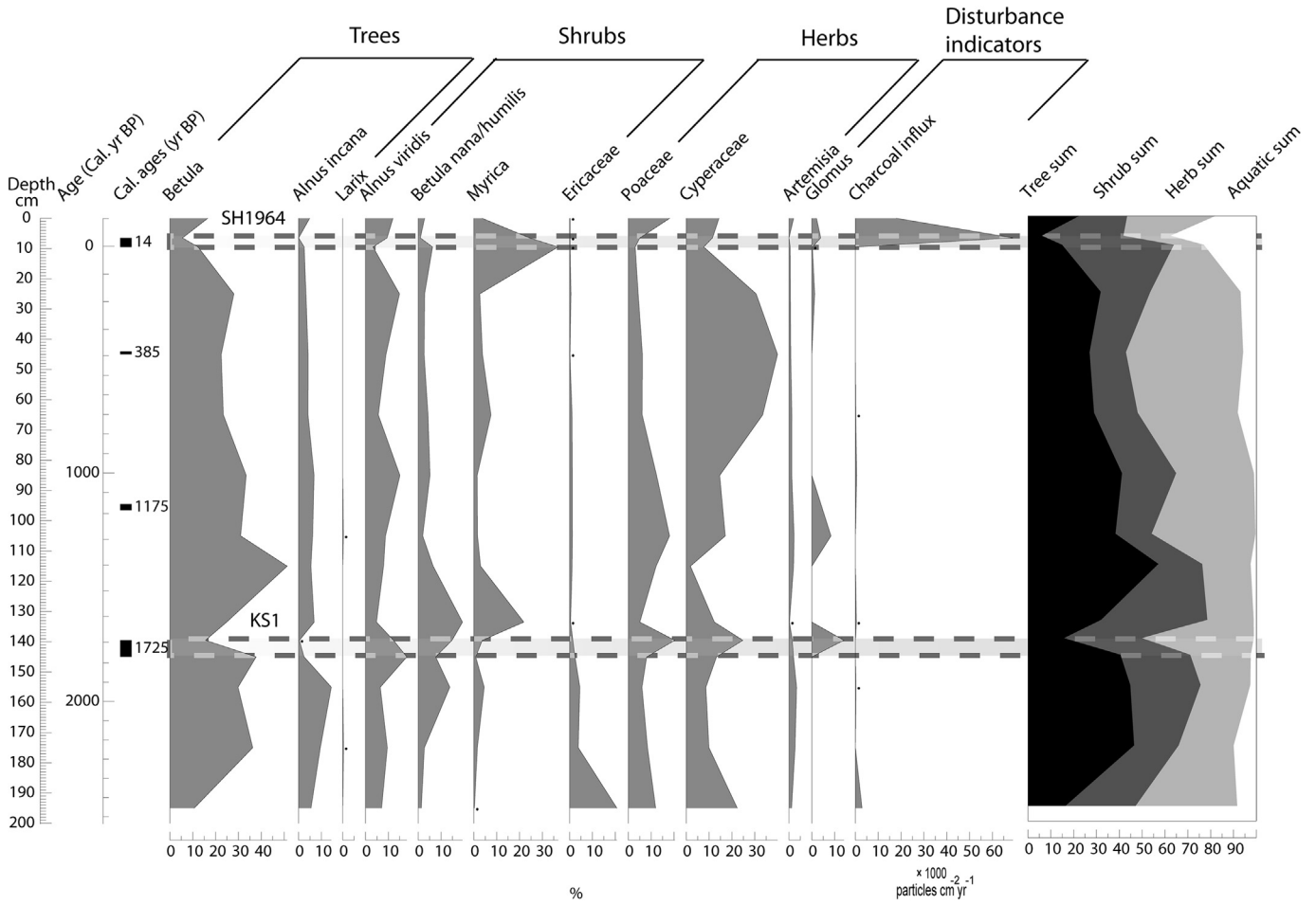

Fig. 5. Pollen percentages and charcoal influx diagram for the last 2500 years of Krutoberegovo wetland (eastern Kamchatka Peninsula, Kamchatsky Krai, Russia) illustrating the impact of the last two major tephra deposition events, KS_1 and SH1964. Selected pollen and spore types only. Aquatic forbs, fern and fern allies, and mosses are excluded from the main sum. Dots represent <0.5% of the main pollen sum. For charcoal influx dots represent <1000 particles cm^{-2} yr^{-1}. Dashed stripes represent the stratigraphic position of the KS_1 (lower) and SH1964 (upper) tephras.

Moreover, our vegetation surveys of the eastern coast, between Ust-Kamchatsk and Stolbovaya Bay (Fig. 1) identified little to no occurrence of *Pinus pumila*, which implies that current climatic conditions favoring a high abundance of *Pinus pumila* communities in western and central Kamchatka are not present on the eastern seaboard.

5.2. The role of volcanic ash falls in vegetation dynamics

The main impacts of volcanic eruptions on terrestrial biota include direct physical damage by tephra falls to the subaerial part of plants and indirect effects such as physical and physiological damage by acid rain due to the volatile compounds ejected in the atmosphere (Eastwood et al., 2002). These impacts are largely felt in the areas proximal to volcanic eruptions although in some cases distal areas are affected as well, mainly through the deposition of acidic aerosols (e.g., Sadler and Grattan, 1999). The direct physical effects on plants are dependent on the frequency of tephra fall events and the thickness of deposits (Lotter and Birks, 1993; Barker et al., 2000). Modern eruptions such as the one of Mount St. Helens in 1980 (Mack, 1981) offer insights into the type and intensity of physical damage to terrestrial vegetation. In the case of the Mount St Helens eruption, Mack (1981) reports that outside the actual blast zone impacts on vegetation were minor and mostly dependent on plant morphology. Ash coating on leaves was usually washed off after the first rain. Grasses and other plants with slender long leaves were the least affected, while prostrate plants or those with clasping leaves suffered most. Paleoecological studies in areas with ancient eruptions such as the "Minoan" eruption of Santorini volcano in the mid second millennium BC (Eastwood et al., 2002) or that of Taupo volcano in New Zealand in 1750 cal yr BP (Wilmshurst and McGlone, 1996; Stott et al., 1998) echo the finds presented in the case of Mount St Helens. The Taupo eruption and the subsequent tephra deposition, while driving major vegetation changes in the area adjacent to the eruption (160 km radius) such as generalized forest die-out and forest fires, had only minor effects in distal areas. In the case of the Santorini eruption (Eastwood et al., 2002) the impact of tephra deposition on terrestrial vegetation in a distal lake catchment, 400 km from the volcano, was only a slight increase in grasses (Poaceae) and possibly sedges (Cyperaceae). A similar increase in Poaceae and Cyperaceae was also reported by Birks and Lotter (1994) and Lotter et al. (1995) in their studies on the environmental effects of the Laacher See eruption during the Late Glacial.

Previous vegetation reconstructions in Kamchatka found little evidence of tephra impact on vegetation (Andrén et al., 2015; Self et al., 2015). For instance, in a 10,000-year record from Pechora Lake, Andrén et al. (2015) identified seven tephra layers of which only one seems to have affected vegetation communities. This event was dated to ca. 6300 cal yr BP and is marked by a minor

increase in grasses (Poaceae), changes in lake geochemistry, and shifts in diatom and chironomid community structures.

At Krutoberegovo the only consistent changes in terrestrial vegetation following tephra deposition are an increase in the proportion of grasses (Poaceae), a decrease in the frequency of tree birch (*Betula*) pollen (Figs. 3 and 5) and in some cases an increase in rate-of-change values (Fig. 3). It should be noted, however, that the decrease in tree birch (*Betula*) pollen may be an artifact of the increase in Poaceae, which could cause other taxa to exhibit proportionally lower frequencies. Other potential impacts that appear to be less frequent or isolated are the increase in sedges (Cyperaceae), shrub alder (*Alnus viridis*), and disturbance indicators (*Glomus* spores and micro-charcoal). The latter may indicate the occurrence of soil erosion and fire following tephra deposition. The most vivid examples illustrating these impacts are the deposition of the last two major tephra layers, KS_1 dated at 1725 cal yr BP and SH1964 from AD 1964 (Table 2 and Fig. 5). In the case of the KS_1 tephra, the immediate effects on vegetation were an increase in grasses (Poaceae), sedges (Cyperaceae), and *Glomus* spores and a decrease in tree and shrub pollen frequencies. In the case of the AD 1964 eruption of the Shiveluch volcano that deposited the SH1964 tephra, the immediate effects seem to be only a decrease in tree (mainly *Betula*) and shrub pollen and an increase in micro-charcoal, followed by the recovery of these taxa and a slight increase in grasses (Poaceae) and sedges (Cyperaceae) (Fig. 5). These changes suggest that the Shiveluch eruption – a volcano situated only 150 km west of Krutoberegovo - may have had a stronger influence on the vegetation than the KS_1 eruption, originating from a volcano situated 700 km to the SW (Fig. 1). Given the relative proximity of the Shiveluch volcano to the sampling site at Krutoberegovo, the eruption in AD 1964 may have resulted in partial *Betula* forest die-out and subsequent forest fires, followed by forest recovery and a slight increase in grassland ecosystems. The mechanism related to the potential forest die-out remains unknown but it could have been caused by acid rain related to the eruption of volcanic aerosols.

6. Conclusions

The Late Glacial to Holocene pollen and charcoal record from Krutoberegovo on Kamchatka's eastern seaboard reveals a complex pattern of vegetation and landscape dynamics which was, for the most part, related to climate variability. The effects of tephra falls on vegetation was short lived and mainly related to expansion of graminoid ecosystems (Poaceae and Cyperaceae) and possibly forest die-out. Our interpretation of the environmental development of eastern Kamchatka based on palynological analysis of the Krutoberegovo peat basin can be summarised as follows:

- The Late Glacial period shows close similarities with the northeastern Pacific coast, in particular southwestern Alaska, and is defined by a warm continental climate briefly interrupted by a cold reversal, the latter being attributed to the quasi-global climate event known as the Younger Dryas or GS1.
- The Early Holocene is marked by a rather modest climate amelioration which favored grasses, alder shrubs, and fern communities, while forest species remained almost absent. After 9200 cal yr BP vegetation communities diversified, probably under the influence of a warmer, oceanic climate, which induced maximum expansion of shrubs and the appearance of the first postglacial forests dominated by alder.
- Between 7000 and 4500 cal yr BP shrublands underwent a generalized collapse in favor of graminoid communities, while the alder forests were progressively replaced by birch. The expansion of birch forests was cut short around 4500 cal yr BP, probably under the influence of climate cooling.
- Between 3000 and 1500 cal yr BP birch forest re-expanded, suggesting an episode of climate amelioration during a generally cool and wet Late Holocene. The present-day landscapes were established ca. 1500 years ago and are characterized by decreasing birch forest cover, shrub alder thickets, and mosaic of grasslands and fens dominated by sedges and bayberry.

Acknowledgements

The authors would also like to thank the National Science Foundation, Grant Award# 0915131, Ezra B. Zubrow P.I., for funding the ICCAP project. Ponomareva and Portnyagin acknowledge support from the Russian Science Foundation grant #16-17-10035. Pendea would like to thank NSERC and Lakehead University for their financial support in the form of two SRC NSERC seed grants. Our sincerest gratitude to all our American and Russian colleagues, postdoctoral scholars, graduate and undergraduate students involved in the lab and fieldwork for this project. The authors would also like to thank two anonymous reviewers for their suggestions that significantly improved the manuscript.

References

Anderson, P.M., Edwards, M.E., Brubaker, L.B., 2003. Results and paleoclimate implications of 35 years of paleoecological research in Alaska. Dev. Quat. Sci. 1, 427–440.
Anderson, P.M., Lozhkin, A.V., Brubaker, L.B., 2002. Implications of a 24 000-yr palynological record for a Younger Dryas cooling and for boreal forest development in northeastern Siberia. Quat. Res. 57, 325–333.
Anderson, R.S., Homola, R.L., Davis, R.B., Jacobson Jr., G.L., 1984. Fossil remains of the mycorrhizal fungal *Glomus fasciculatum* complex in postglacial lake sediments from Maine. Can. J. Bot. 62 (11), 2325–2328.
Andrén, E., Klimaschewski, A., Self, A.E., Amour, N.S., Andreev, A.A., Bennett, K.D., Conley, D.J., Edwards, T.W., Solovieva, N., Hammarlund, D., 2015. Holocene climate and environmental change in north-eastern Kamchatka (Russian Far East), inferred from a multi-proxy study of lake sediments. Glob. Planet. Change 134, 41–54.
Barker, P.A., Telford, R., Merdaci, O., Williamson, D., Taieb, M., Vincens, A., Gibert, E., 2000. The sensitivity of a Tanzanian crater lake to catastrophic tephra input and four millennia of climate change. Holocene 10, 303–310.
Bartlein, P.J., Harrison, S.P., Brewer, S., Connor, S., Davis, B.A.S., Gajewski, K., Guiot, J., Harrison-Prentice, T.I., Henderson, A., Peyron, O., Prentice, I.C., 2011. Pollen-based continental climate reconstructions at 6 and 21 ka: a global synthesis. Clim. Dyn. 37 (3–4), 775–802.
Bennett, K.D., 1996. Determination of the number of zones in a biostratigraphical sequence. New Phytol. 132 (1), 155–170.
Bennett, K.D., 2009. 'Psimpoll'and 'Pscomb': C Programs for Analysing Pollen Data and Plotting Pollen Diagrams (Version 4.27). Available online from:. Queen's University Quaternary Geology program http://www.chrono.qub.ac.uk/psimpoll.html/ (Accessed 10 May 2016).
Berger, A.L., 1978. Long-term variations of daily insolation and Quaternary climatic changes. J. Atmos. Sci. 35 (12), 2362–2367.
Birks, H., Berglund, B.E., 1979. Holocene pollen stratigraphy of southern Sweden: a reappraisal using numerical methods. Boreas 8 (3), 257–279.
Birks, H.J.B., 1968. The identification of *Betula nana* pollen. New Phytol. 67, 309–314.
Birks, H.J.B., 1986. Numerical zonation, comparison and correlation of Quaternary pollen-stratigraphical data. In: Berglund, B. (Ed.), Handbook of Holocene Palaeoecology and Palaeohydrology. Wiley, New York, pp. 743–774.
Birks, H.J.B., Lotter, A.F., 1994. The impact of the Laacher See volcano (11,000 yr BP) on terrestrial vegetation and diatoms. J. Paleolimnol. 11, 313–322.
Björck, S., Walker, M.J.C., Cwynar, L.C., et al., 1998. An event stratigraphy for the Last Termination in the North Atlantic region based on the Greenland ice-core record: a proposal by the INTIMATE group. J. Quat. Sci. 13, 283–292.
Blaauw, M., Christen, J.A., 2011. Flexible paleoclimate age-depth models using an autoregressive gamma process. Bayesian Anal. 6 (3), 457–474.
Blackmore, S., Steinmann, J.A., Hoen, P.P., Punt, W., 2003. Betulaceae and Corylaceae. Rev. Palaeobot. Palynol. 123 (1), 71–98.
Braitseva, O.A., Melekestsev, Sulerzhitsky, L.D., 2005. New data on the Pleistocene deposits age in the central Kamchatka depression. Stratigr. Geol. 13 (1), 99–107.
Braitseva, O.A., Ponomareva, V.V., Sulerzhitsky, L.D., Melekestsev, I.V., Bailey, J., 1997. Holocene key-marker tephra layers in Kamchatka, Russia. Quat. Res. 47, 125–139.
Braitseva, O.A., Melekestsev, I.V., Ponomareva, V.V., Kirianov, V. Yu, 1996. The caldera-forming eruption of Ksudach volcano about cal. AD 240, the greatest explosive event of our era in Kamchatka. J. Volcanol. Geotherm. Res. 70 (1–2),

49–66.
Brubaker, L.B., Anderson, P.M., Murray, B.M., Koon, D., 1998. A palynological investigation of true-moss (Bryidae) spores: morphology and occurrence in modern and late Quaternary lake sediments of Alaska. Can. J. Bot. 76, 2145–2157.
Brubaker, L.B., Anderson, P.M., Hu, F.S., 2001. Vegetation ecotone dynamics in southwest Alaska during the Late Quaternary. Quat. Sci. Rev. 20 (1), 175–188.
Caseldine, C., 2001. Changes in *Betula* in the Holocene record from Iceland—a palaeoclimatic record or evidence for early Holocene hybridisation? Rev. Palaeobot. Palynol. 117 (1), 139–152.
Clegg, B.F., Tinner, W., Gavin, D.G., Hu, F.S., 2005. Morphological differentiation of *Betula* (birch) pollen in northwest North America and its palaeoecological application. Holocene 15 (2), 229–237.
Dirksen, V., Dirksen, O., Diekmann, B., 2013. Holocene vegetation dynamics and climate change in Kamchatka Peninsula. Russ. Far East. Rev. Palaeobot. Palynol. 190, 48–65.
Elias, S.A., Short, S.K., Birks, H.H., 1997. Late Wisconsin environments of the Bering land bridge. Palaeogeogr. Palaeoclim. Palaeoecol. 136 (1), 293–308.
Eastwood, W.J., Tibby, J., Roberts, N., Birks, H.J.B., Lamb, H.F., 2002. The environmental impact of the Minoan eruption of Santorini (Thera): statistical analysis of palaeoecological data from Golbisar, southwest Turkey. Holocene 12 (4), 431–444.
Eichelberger, J., Gordeev, E., Kasahara, M., Izbekov, P., Lees, J., 2007–2016. Volcanism and Subduction: the Kamchatka Region, American Geophysical Union Geophysical Monograph Series, vol. 172. Eijkelkamp Inc.. Eijkelkamp Gouge Augers Manual. https://en.eijkelkamp.com/products/augering-soil-sampling-equipment/bi-partite-gouge-auger-set-sa.html/ (Accessed 10 August 2016).
Faegri, K., Kaland, P.E., Krzywinski, K., 1989. Textbook of Pollen Analysis, fourth ed. John Wiley & Sons, Chichester.
Finsinger, W., Tinner, W., 2005. Minimum count sums for charcoal concentration estimates in pollen slides: accuracy and potential errors. Holocene 15 (2), 293–297.
Grimm, E.C., 1987. CONISS: a FORTRAN 77 program for stratigraphically constrained cluster analysis by method of incremental sum of squares. Comp. Geosci. 13, 13–35.
Gorshkov, G.S., Dubik, Yu M., 1970. Gigantic directed blast at Shiveluch volcano (Kamchatka). Bull. Volcanol. 34, 261–288.
Hammarlund, D., Klimaschewski, A., Amour, N.A.S., Andrén, E., Self, A.E., Solovieva, N., Andreev, A.A., Barnekow, L., Edwards, T.W., 2015. Late Holocene expansion of Siberian dwarf pine (*Pinus pumila*) in Kamchatka in response to increased snow cover as inferred from lacustrine oxygen-isotope records. Glob. Planet. Change 134, 91–100.
Hoff, U., Dirksen, O., Dirksen, V., Kuhn, G., Meyer, H., Diekmann, B., 2014. Holocene freshwater diatoms: palaeoenvironmental implications from south Kamchatka, Russia. Boreas 43, 22–41.
Igarashi, Y., Zharov, A.E., 2011. Climate and vegetation change during the late Pleistocene and early Holocene in Sakhalin and Hokkaido, northeast Asia. Quat. Int. 237 (1), 24–31.
Ives, J.W., 1977. Pollen separation of three North American birches. Arct. Alp. Res. 73–80.
Jacobson Jr., G.L., Grimm, E.C., 1988. Synchrony of rapid change in late-glacial vegetation south of the Laurentide ice sheet. Bull. Buffalo Soc. Nat. Sci. 33, 31–38.
Jacobson Jr., G.L., Webb III, T., Grimm, E.C., 1987. Patterns and rates of vegetation change during the deglaciation of eastern North America. In: Ruddiman, W.F., Wright Jr., H.E. (Eds.), North America and Adjacent Oceans during the Last Deglaciation. Geological Society of America, Boulder, pp. 277–288.
Jankovská, V., Andreev, A.A., Panova, N.K., 2006. Holocene environmental history on the eastern slope of the Polar Ural Mountains, Russia. Boreas 35 (4), 650–661.
Kapp, R.O., Davis, O.K., King, J.E., 2000. Ronald O. Kapp's Pollen and Spores, second ed. American Association of Stratigraphic Palynologists.
Kaufman, D.S., Ager, T.A., Anderson, N.J., Anderson, P.M., Andrews, J.T., Bartlein, P.J., Brubaker, L.B., Coats, L.L., Cwynar, L.C., Duvall, M.L., Dyke, A.S., 2004. Holocene thermal maximum in the western Arctic (0–180 W). Quat. Sci. Rev. 23 (5), 529–560.
Keigwin, L.D., Donnelly, J.P., Cook, M.S., Driscoll, N.W., Brigham-Grette, J., 2006. Rapid sea-level rise and Holocene climate in the Chukchi sea. Geol. 34 (10), 861–864.
Khotinsky, N.A., 1977. Holocene of the Northern Eurasia. Nauka, Moscow (In Russian).
Klimaschewski, A., 2010. Late Quaternary Environmental Change of Kamchatka. Doctoral Thesis. School of Geography, Archaeology, and Palaeoecology, Queen's University, Belfast.
Kokorowski, H.D., Anderson, P.M., Mock, C.J., Lozhkin, A.V., 2008. A re-evaluation and spatial analysis of evidence for a Younger Dryas climatic reversal in Beringia. Quat. Sci. Rev. 27 (17), 1710–1722.
Kondratyuk, V.I., 1974. Klimat Kamchatki (Climate of Kamchatka). Hydrometeoizdat, Moscow (In Russian).
Krestov, P.V., 2008. Forest vegetation of easternmost Russia (Russian Far East). In: Kolbek, J., et al. (Eds.), Forest Vegetation of Northeast Asia. Kluwer Academic Publishers, Amsterdam, pp. 93–180.
Kyle, Ph R., Ponomareva, V.V., Rourke Schluep, R., 2011. Geochemical characterization of marker tephra layers from major Holocene eruptions in Kamchatka, Russia. Int. Geol. Rev. 53 (9), 1059–1097.
Lotter, A.F., Birks, H.J.B., 1993. The impact of the Lacher See tephra on terrestrial and aquatic ecosystems in the Black Forest, southern Germany. J. Quat. Sci. 8, 263–276.
Lotter, A.F., Birks, H.J.B., Zolitschka, B., 1995. Late-glacial pollen and diatom changes in response to two different environmental perturbations: volcanic eruption and Younger Dryas cooling. J. Paleolimnol. 14, 23–47.
Lozhkin, A.V., Anderson, P., Eisner, W.R., Solomatkina, T.B., 2011a. Late glacial and Holocene landscapes of central Beringia. Quat. Res. 76 (3), 383–392.
Lozhkin, A.V., Anderson, P.M., Eisner, W.R., Ravako, L.G., Hopkins, D.M., Brubaker, L.B., Colinvaux, P.A., Miller, M.C., 1993. Late Quaternary lacustrine pollen records from southwestern Beringia. Quat. Res. 39 (3), 314–324.
Lozhkin, A.V., Anderson, P.M., Vartanyan, S.L., Brown, T.A., Belaya, B.V., Kotov, A.N., 2001. Late Quaternary paleoenvironments and modern pollen data from Wrangel Island (Northern Chukotka). Quat. Sci. Rev. 20 (1), 217–233.
Lozhkin, A.V., Anderson, P.M., Vazhenina, L.N., 2011b. Younger Dryas and early Holocene peats from northern far East Russia. Quat. Int. 237 (1), 54–64.
Mack, R.N., 1981. Initial effects of ashfall from Mount St Helens on vegetation in Eastern Washington and adjacent Idaho. Science 213, 537–539.
Mäkelä, E.M., 1996. Size distinctions between *Betula* pollen types—a review. Grana 35 (4), 248–256.
Mann, D.H., Hamilton, T.D., 1995. Late Pleistocene and Holocene paleoenvironments of the North Pacific coast. Quat. Sci. Rev. 14 (5), 449–471.
Mathewes, R.W., 1993. Evidence for Younger Dryas-age cooling on the North Pacific coast of America. Quat. Sci. Rev. 12 (5), 321–331.
Max, L., Riethdorf, J.R., Tiedemann, R., Smirnova, M., Lembke-Jene, L., Fahl, K., Nürnberg, D., Matul, A., Mollenhauer, G., 2012. Sea surface temperature variability and sea-ice extent in the subarctic northwest Pacific during the past 15,000 years. Paleoceanogr 27 (3), PA3213. http://dx.doi.org/10.1029/2012PA002292.
Meyer, H., Chapligin, B., Hoff, U., Nazarova, L., Diekmann, B., 2014. Oxygen isotope composition of diatoms as Late Holocene climate proxy at Two-Yurts Lake, central Kamchatka, Russia. Glob. Planet. Change 134, 118–128.
Mock, C.J., Bartlein, P.J., Anderson, P.M., 1998. Atmospheric circulation patterns and spatial climatic variation in Beringia. Int. J. Climatol. 10, 1085–1104.
Moore, P.D., Webb, J.A., Collison, M.E., 1991. Pollen Analysis. Blackwell Scientific Publications, Oxford.
Nazarova, L., de Hoog, V., Hoff, U., Dirksen, O., Diekmann, B., 2013. Late Holocene climate and environmental changes in Kamchatka inferred from the subfossil chironomid record. Quat. Sci. Rev. 67, 81–92.
Neishtadt, M.I., 1957. Forests History and Paleogeography of the USSR in the Holocene. Nauka, Moscow (In Russian).
Neulieb, T., Levac, E., Southon, J., Lewis, M., Pendea, I.F., Chmura, G.L., 2013. Potential pitfalls of pollen dating. Radiocarbon 55 (2–3), 1142–1155.
Pendea, I.F., Harmsen, H., Keeler, D., Zubrow, E.B., Korosec, G., Ruhl, E., Ponkratova, I., Hulse, E., 2016. Prehistoric human responses to volcanic tephra fall events in the Ust-Kamchatsk region, Kamchatka Peninsula (Kamchatsky Krai, Russian Federation) during the middle to late Holocene (6000–500 cal BP). Quat. Int. 394, 51–68.
Peteet, D., 1995. Global Younger Dryas? Quat. Int. 28, 93–104.
Peteet, D.M., Daniels, R.A., Heusser, L.E., Vogel, J.S., Southon, J.R., Nelson, D.E., 1993. Late-glacial pollen, macrofossils and fish remains in northeastern USA—the Younger Dryas oscillation: a contribution to the 'North Atlantic seaboard programme'of IGCP253,'Termination of the Pleistocene'. Quat. Sci. Rev. 12 (8), 597–612.
Peteet, D.M., Mann, D.H., 1994. Late-glacial vegetational, tephra, and climatic history of southwestern Kodiak Island, Alaska. Ecoscience 255–267.
Pevzner, M.M., Ponomareva, V.V., Melekestsev, I.V., 1998. Chernyi Yar - reference section of the Holocene ash markers at the northeastern coast of Kamchatka. Volcanol. Seismol. 19 (4), 389–406.
Pinegina, T.K., Bourgeois, J., Kravchunovskaya, E.A., Lander, A.V., Arcos, M.E., Pedoja, K., MacInnes, B.T., 2013. A nexus of plate interaction: vertical deformation of Holocene wave-built terraces on the Kamchatsky Peninsula (Kamchatka, Russia). Geol. Soc. Am. Bull. 125 (9–10), 1554–1568.
Plunkett, G., Coulter, S.E., Ponomareva, V.V., Blaauw, M., Klimaschewski, A., Hammarlund, D., 2015. Distal tephrochronology in volcanic regions: Challenges and insights from Kamchatkan lake sediments. Glob. Planet. Change 134, 26–40.
Ponomareva, V., Portnyagin, M., Derkachev, A., Pendea, I.F., Bourgeois, J., Reimer, P.J., Garbe-Schönberg, D., Krasheninnikov, S., Nürnberg, D., 2013. Early Holocene M~6 explosive eruption from Plosky volcanic massif (Kamchatka) and its tephra as a link between terrestrial and marine paleoenvironmental records. Int. J. Earth Sci. 102 (6), 1673–1699.
Ponomareva, V., Portnyagin, M., Pevzner, M., Blaauw, M., Kyle, Ph, Derkachev, A., 2015. Tephra from andesitic Shiveluch volcano, Kamchatka, NW Pacific: chronology of explosive eruptions and geochemical fingerprinting of volcanic glass. Int. J. Earth Sci. Geol. Rundsch. 104, 1459–1482.
Praetorius, S.K., Mix, A.C., 2014. Synchronization of North Pacific and Greenland climates preceded abrupt deglacial warming. Science 345 (6195), 444–448.
Prentice, I.C., 1981. Quantitative birch (*Betula* L.) pollen separation by analysis of size frequency data. New Phytol. 89 (1), 145–157.
Punt, W., Hoen, P.P., 2009. the northwest European pollen flora, 70: Asteraceae/Asteroideae. Rev. Palaeobot. Palynol. 157 (1), 22–183.
Rasmussen, S.O., Andersen, K.K., Svensson, A.M., Steffensen, J.P., Vinther, B.M., Clausen, H.B., Siggaard-Andersen, M.L., Johnsen, S.J., Larsen, L.B., Dahl-Jensen, D., Bigler, M., 2006. A new Greenland ice core chronology for the last glacial termination. J. Geophys. Res. Atmos. 111 (D6) (1984–2012).
Reimer, P.J., Bard, E., Bayliss, A., Beck, J.W., Blackwell, P.G., Bronk Ramsey, C.,

Buck, C.E., Cheng, H., Edwards, R.L., Friedrich, M., Grootes, P.M., Guilderson, T.P., Haflidason, H., Hajdas, I., Hatt_e, C., Heaton, T.J., Hoffmann, D.L., Hogg, A.G., Hughen, K.A., Kaiser, K.F., Kromer, B., Manning, S.W., Niu, M., Reimer, R.W., Richards, D.A., Scott, E.M., Southon, J.R., Staff, R.A., Turney, C.S.M., van der Plicht, J., 2013. IntCal13 and Marine13 radiocarbon age calibration curves 0-50,000 years cal BP. Radiocarbon 55 (4), 1869–1887.

Renssen, H., Seppä, H., Crosta, X., Goosse, H., Roche, D.M., 2012. Global characterization of the Holocene thermal maximum. Quat. Sci. Rev. 48, 7–19.

Sadler, J.P., Grattan, J.P., 1999. Volcanoes as agents of environmental change. Glob. Planet. Change 21, 181–196.

Self, A.E., Klimaschewski, A., Solovieva, N., Jones, V.J., Andrén, E., Andreev, A.A., Hammarlund, D., Brooks, S.J., 2015. The relative influences of climate and volcanic activity on Holocene lake development inferred from a mountain lake in central Kamchatka. Glob. Planet. Change 134, 67–81.

Stockmarr, J., 1977. Tablets with spores used in absolute pollen analysis. Pollen Spores 13, 615–621.

Stott, P., Horrocks, M., Ogden, J., 1998. The effects of the Taupo Tephra eruption of c. 1718 BP on the vegetation of Mt Hauhungatahi, central North Island, New Zealand. J. Biogeog 25 (4), 649–660.

Talma, A.S., Vogel, J.C., 1993. A simplified approach to calibrating (super 14) C dates. Radiocarbon 35 (2), 317–322.

Tarasov, P.E., Webb III, T., Andreev, A.A., Afanas' Eva, N.B., Berezina, N.A., Bezusko, L.G., Blyakharchuk, T.A., Bolikhovskaya, N.S., Cheddadi, R., Chernavskaya, M.M., Chernova, G.M., 1998. Present-day and mid-Holocene biomes reconstructed from pollen and plant macrofossil data from the former Soviet Union and Mongolia. J. Biogeogr. 25 (6), 1029–1053.

Tinner, W., Hu, F.S., 2003. Size parameters, size-class distribution and area-number relationship of microscopic charcoal: relevance for fire reconstruction. Holocene 13 (4), 499–505.

Walker, M.J.C., Berkelhammer, M., Björck, S., Cwynar, L.C., Fisher, D.A., Long, A.J., Lowe, J.J., Newnham, R.M., Rasmussen, S.O., Weiss, H., 2012. Formal subdivision of the Holocene series/Epoch: a discussion paper by a working group of INTIMATE (Integration of ice-core, marine and terrestrial records) and the subcommission on Quaternary stratigraphy (International Commission on stratigraphy). J. Quat. Sci. 27 (7), 649–659.

Wilmshurst, J.M., McGlone, M.S., 1996. Forest disturbance in the central North Island, New Zealand, following the 1850 BP Taupo eruption. Holocene 6, 399–411.

Yakubov, V., 2007. Plants of Kamchatka (The Field Guide). Way, Truth and Life Press, Moscow (In Russian and English).

Yasuhara, M., Hunt, G., Cronin, T.M., Hokanishi, N., Kawahata, H., Tsujimoto, A., Ishitake, M., 2012. Climatic forcing of Quaternary deep-sea benthic communities in the North Pacific Ocean. Paleobiol. 38 (1), 162–179.